Design and fabrication of 45° inclined mirrors for wafer-level optical absorption spectroscopy

Ayerden, N.P.; Ghaderi, M.; Wolffenbuttel, R.F.

DOI
10.1088/1742-6596/757/1/012018

Publication date
2016

Document Version
Final published version

Published in
Journal of Physics: Conference Series

Citation (APA)
Ayerden, N. P., Ghaderi, M., & Wolffenbuttel, R. F. (2016). Design and fabrication of 45° inclined mirrors for wafer-level optical absorption spectroscopy. *Journal of Physics: Conference Series*, *757*(1), 1-6. Article 012018. https://doi.org/10.1088/1742-6596/757/1/012018

Design and fabrication of 45° inclined mirrors for wafer-level optical absorption spectroscopy

2016 J. Phys.: Conf. Ser. 757 012018

(http://iopscience.iop.org/1742-6596/757/1/012018)

Design and fabrication of 45° inclined mirrors for wafer-level optical absorption spectroscopy

N P Ayerden, M Ghaderi and R F Wolffenbuttel

Faculty of EEMCS, Delft University of Technology, Mekelweg 4, 2628 CD, Delft, Netherlands

E-mail: n.p.ayerden@tudelft.nl

Abstract. The increasing demand for small, robust and low-cost gas sensors triggers the batch fabrication of highly selective and sensitive miniaturized devices. A linear variable optical filter (LVOF) based microspectrometer enables selectivity in a wide wavelength range, while maintaining the robustness and low cost. To achieve sensitivity in an LVOF based absorption spectrometer, a long gas cell is required. In this paper, we propose an on-chip absorption path that also serves as a gas cell, where the light beam is steered using 45° inclined mirrors. The fabrication of 45° inclined mirrors is demonstrated and optical efficiency of the system is analyzed using ray tracing.

1. Introduction

The composition measurement of gases is of great importance in a diverse range of applications, such as the assessment of indoor air quality [1, 2], atmospheric studies [3, 4] and breath analysis [5, 6, 7, 8]. The increasing demand for field use provides an incentive for the development of small, robust and low-cost gas sensors.

Optical absorption spectroscopy offers a promising compromise between nonselective and low-cost methods such as pellistors, and high-resolution and high-cost methods such as gas chromatography [9]. An optical absorption based spectrometer is composed of a light source, a wavelength-selective device, a sample cell and a detector. The light is passed through a sample and the ratio of absorbed to incident radiation is recorded. The sample is identified by comparing the acquired spectrum with a database. Thanks to its self-referencing, non-destructive, fast response and high-selectivity properties, optical absorption spectroscopy stands out among other gas sensing methods.

The Beer-Lambert Law states that the attenuation of light (i.e. absorbance) passing through a medium is a linear function of the absorption coefficient and the concentration of the attenuating species in the medium as well as the optical path length [10]. The absorption coefficient is a wavelength-dependent intrinsic property of the sample gas. However, the resolving power of the measurement instrument determines its actual value. The remaining two parameters; the concentration and the optical path length determine the absorbance for a particular instrument resolution. Therefore, at a given detector sensitivity, the low concentration of the sample can be compensated either by a wavelength-selective device with high resolution or a long optical absorption path.

The integration of a miniaturized light source with the LVOF and the detector array enables low-cost microspectroscopy. The sensitivity of such a microspectrometer can be enhanced by

improving the resolution of the filter. However, given the operating principle of the LVOF, a pixel in the detector array must not be wider than the full-width-half-max (FWHM) of the filter. In addition to the constraints on the pixel size imposed by the fabrication tolerances, the inversely proportional relation between the pixel width and the detector sensitivity allows for only limited improvement in the overall sensor sensitivity.

The second parameter that can be used for improving the sensor sensitivity is the length of the optical absorption path. External multipass absorption cells such as White cell [11] and Herriott cell [12] composed of a set of spherical mirrors have been widely used for path length elongation through multiple reflections. An improved configuration known as the circular multipass cell allows a star-shaped trajectory of the light beam [13, 14]. Moreover, the multiple reflections in high-finesse optical cavities can be exploited to elongate the effective optical absorption path [15, 16]. However, the demanding requirements on the alignment and surface profile of the mirrors complicates the actual implementation in miniaturized systems.

An on-chip gas cell, where the light beam is propagated along the surface of the wafer allows for efficient use of space, while improving the sensitivity in wafer-level spectroscopy. Lab-on-a-chip devices with 45° inclined mirrors to steer the beam along the wafer surface have been presented in the literature to analyze fluids with high sensitivity using small sample volumes [17, 18, 19]. However, these devices usually employ a low-cost LED as the light source without a wavelength-selective device, thereby limiting the selectivity of the sensor. Instead, we propose a system that is realized by implementing the absorption path and the optics on one wafer and the light source, the LVOF and the detector array on the other. By bonding these two wafers, a sample cell to trap the gas inside is created. Therefore, the sensitivity of the sensor is improved by the on-chip absorption path, while the selectivity is ensured by the wideband operation of the LVOF at the wafer level. In this paper, the fabrication and the optical efficiency of an on-chip gas cell with 45° inclined mirrors are investigated.

2. Fabrication

The increasing use of waveguides in integrated optical devices necessitated the fabrication of 45° inclined mirrors for efficient coupling. Several methods can be used to fabricate 45° inclined mirrors, such as laser ablation [20], soft molding [21], reactive ion etching [22] and microdicing [23, 24]. Among all these, the method based on photolithography and subsequent wet etching is the most compatible with MEMS fabrication [25].

The fabrication of 45° inclined mirrors can be achieved by aligning the etch mask with the $< 100 >$ direction in a (100) wafer and subsequent anisotropic etching with a surfactant [26, 27, 28]. The mask alignment allows for revealing the {110} planes according to the crystal orientation, while the surfactant improves surface quality of the mirror [29].

The process flow for the fabrication of 45° inclined mirrors is given in Fig. 1(a)-(d). Initially, a 300 nm thick SiN is deposited using LPCVD. To be able to use this layer as a mask during wet etching, a lithography step with 10 mm by 10 mm checker pattern mask is applied. Subsequently, the SiN on the windows is removed by reactive ion etching, using 65 sccm C_2F_6 at an etch rate of approximately 5 nm/s. After the removal of the photoresist in oxygen plasma, the wafer is subjected to wet etching using KOH and TMAH with the surfactant Triton X-100.

The patterned wafer before the wet etching step is shown in Fig. 1(e). The checker pattern is aligned with the $< 100 >$ direction, which is equivalent to rotating the mask for 45° with respect to the primary flat. The crystallographic alignment could be further improved compared to the angular alignment with respect to the primary flat of the wafer by observing pre-etched test structures [30, 31, 32]. However, this was not required in our experiments.

First, wet etching experiments were performed with TMAH, where a solution of 25% TMAH + 200 ppm Triton X-100 at 75 °C was used. 45° inclined mirrors were achieved on the {110} plane at an etch rate of 0.21 µm/min. However, randomly located pyramids were formed on the

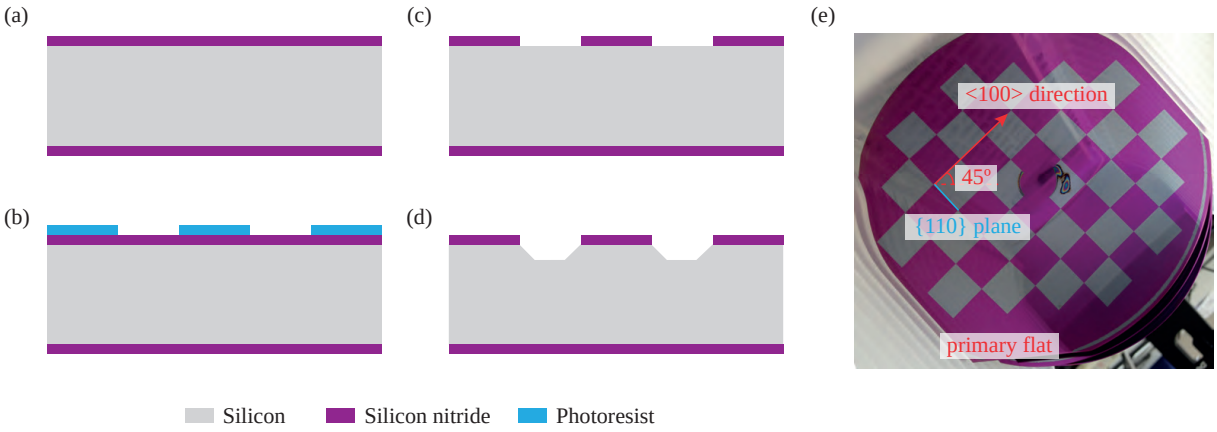

Figure 1. The process flow for the fabrication of 45° inclined mirrors: (a) LPCVD SiN deposition, (b) patterning the SiN mask, (c) plasma etching of the SiN mask and (d) anisotropic etching of silicon. (e) The wafer after lithography and development steps with a 10 mm by 10 mm checker pattern.

{100} plane as shown in Fig. 2. Since these pyramids are on the light path, they could block the light and decrease the throughput. Therefore, a second set of experiments were performed with KOH as the etching agent.

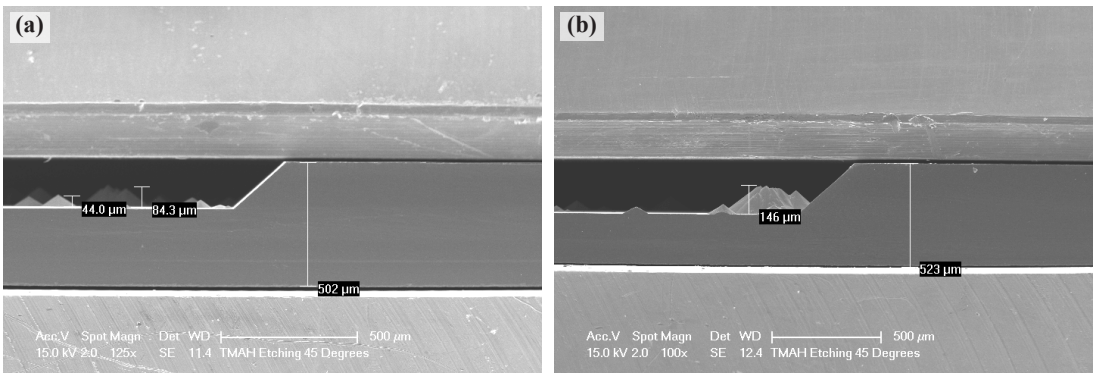

Figure 2. SEM images of 45° inclined mirrors etched (a) 198 µm and (b) 262 µm deep using 25% TMAH + 200 ppm Triton X-100 at 75 C.

For KOH etching, a solution with 2 M KOH + 60 ppm Triton X-100 at 90 °C is prepared. KOH etching with the surfactant Triton X-100 resulted in smooth inclined surfaces as shown in Fig. 3. The etch rate is calculated as 0.10 µm/min. In contrast to the partial blockage in TMAH etching, the KOH etching resulted in roughness-free {100} planes, thereby allowing a light path without randomly formed structures.

The surface roughness of the etched mirrors are measured using atomic-force microscopy. The mirrors are diced along the edges and placed on a 45° inclined wedge to obtain a flat surface for roughness analysis. The measured root-mean-square (RMS) roughness values are below 15 nm, safely within the optical flatness limit of $\lambda/10$, even in the UV band of the spectrum.

3. Optical Efficiency Analysis

The power efficiency of a system with 45° inclined mirrors is analyzed using the ray tracing software, Zemax. The simplified system is composed of a light source, two 45° inclined mirrors

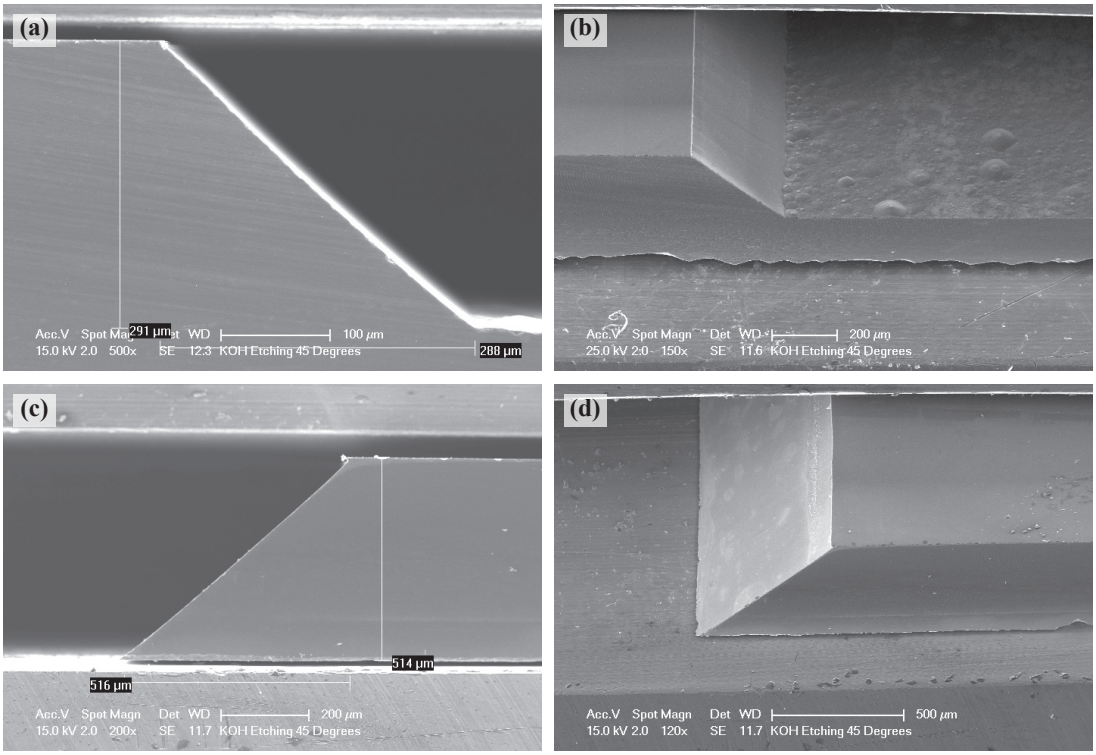

Figure 3. SEM images of 45° inclined mirrors etched (a, b) 290 µm deep and (c, d) through the Si wafer using 2 M KOH + 60 ppm Triton X-100 at 90 °C.

with a 10 mm long optical light path in-between and an image plane as shown in Fig. 4. The light source is implemented as a cylindrical lens to realize a filament-like emitter. The cylindrical lens is designed as a toroidal surface with infinite radius of rotation. The diameter of the cylinder is 0.06 mm, while the length is 3 mm. The size of the entrance pupil diameter is selected as 3 mm so that the entire cylindrical lens surface is illuminated. The size of the 45° inclined mirrors is maximized to demonstrate the best-case efficiency. The largest mirror can be achieved by through-wafer etching. Therefore, the width of the mirror is selected as 0.74 mm assuming a standard 4" wafer thickness of 524 µm. The cylindrical lens and the image plane are placed 0.5 mm away from the mirrors.

Geometric image analysis in the sequential mode of Zemax is used for power simulations. This type of analysis assumes a unit power of 1 W at the initial surface and calculates the power distribution at every surface based purely on geometrical optics. Power analysis results for the system with 45° inclined mirrors are given in Fig. 5. Since the cylindrical lens is the light source in the actual implementation, the power at the image plane is normalized to the power at the cylindrical lens rather than the entrance pupil. This results in the best-case power efficiency of 1.1%. However, through-wafer etching, despite maximizing power efficiency, impairs the robustness of the entire system. Moreover, the stray light that does not follow the predefined optical path makes the quantitative material identification, which highly depends on the length of the optical absorption path, unreliable. In addition, the fabrication tolerances could easily decrease the efficiency below 1.1%, which is undesirable in systems with low-power wideband emitters. Therefore, an on-chip gas cell with 45° inclined mirrors must be combined with collimating optics.

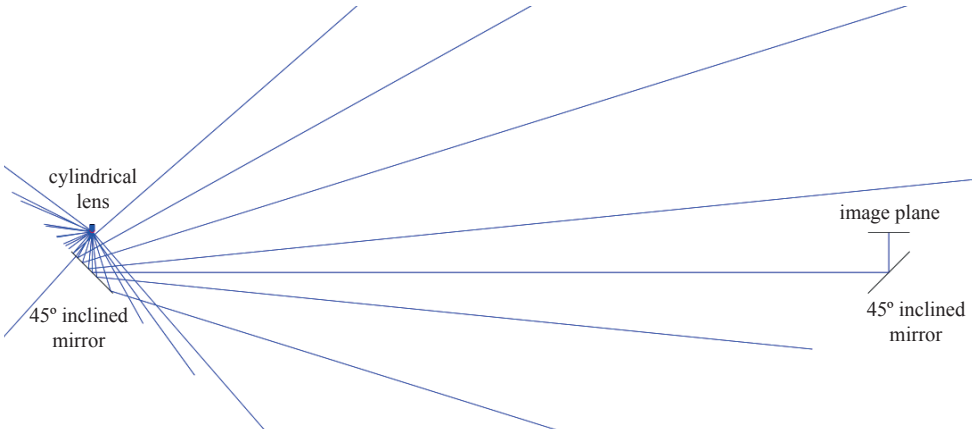

Figure 4. Zemax layout of the design with 45° inclined mirrors.

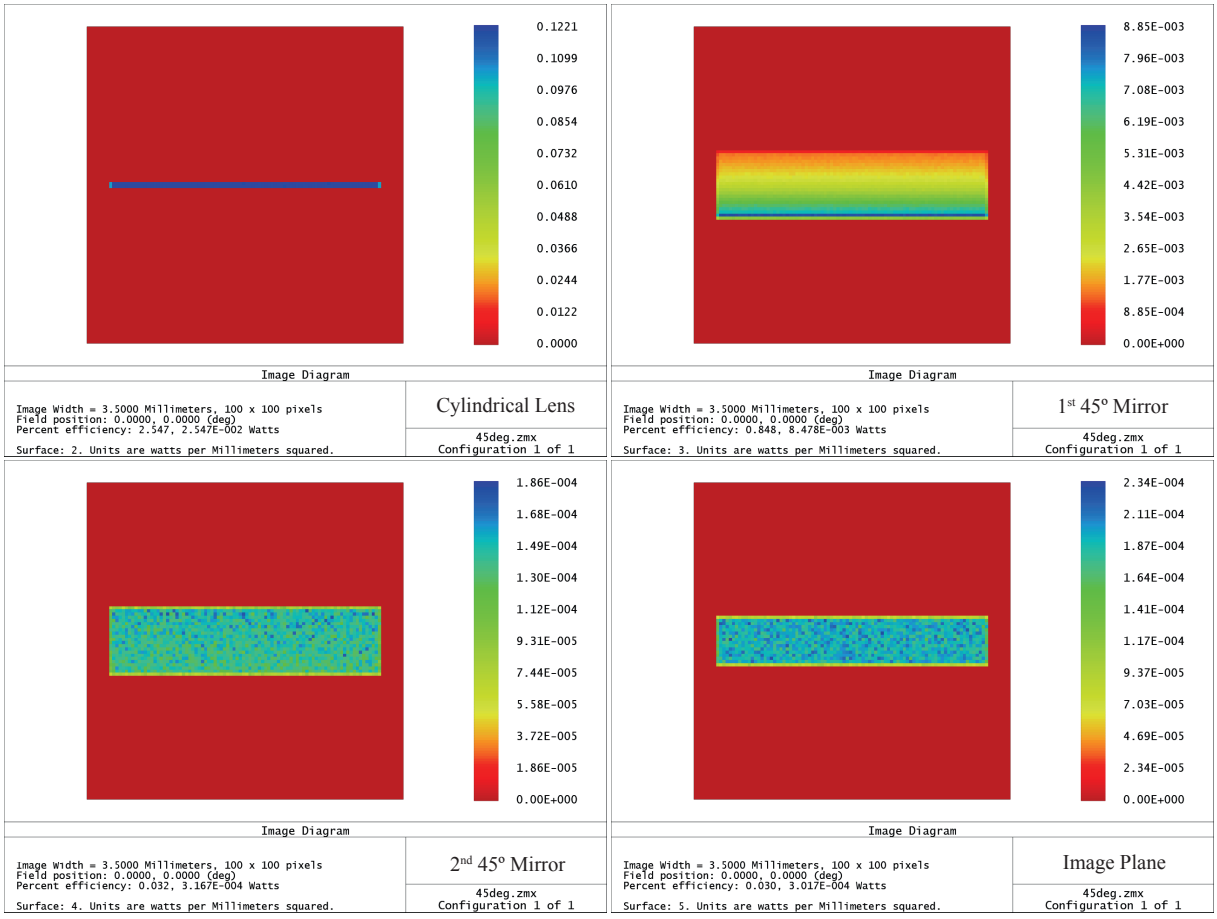

Figure 5. Power analysis results of the design with 45° inclined mirrors.

4. Conclusions

The feasibility of an on-chip absorption path with 45° inclined mirrors is investigated in terms of fabrication and optical efficiency. 45° inclined mirrors are realized by aligning the mask with the $< 100 >$ direction in a (100) wafer and subsequent anisotropic etching. The surfactant Triton X-100 is added to the wet etching solution to improve the surface quality of the mirrors.

Experiments with KOH and TMAH solutions resulted in an RMS surface roughness of less than 15 nm, while randomly located pyramids were formed on the {100} plane in TMAH etching. Optical efficiency of the on-chip absorption path with 45° inclined mirrors is analyzed using ray tracing in Zemax. The results imply that without collimating and focusing optics, the optical throughput is 1.1% in the best-case scenario. The fabrication of lenses on the light source and the LVOF to collimate and focus the light respectively, further complicates the process and puts an imbalance on the fabrication complexity between the top and the bottom wafers. Therefore, instead of steering the light beam with 45° inclined mirrors, off-axis parabolic mirrors can be employed to both steer and collimate or focus the light. Fabrication of such aspherical optical components have been previously presented in the literature [33, 34]. As a result, by integrating the wafer with the mirrors and the optical absorption path to the wafer with the light source, the LVOF and the detector array, a highly sensitive and selective microspectrometer can be built at the wafer-level.

References

[1] Kostiainen R 1995 *Atmos. Environ.* **29** 693–702
[2] Pushkarsky M B, Webber M E and Patel C K N 2003 *Appl. Phys. B-Lasers O.* **77** 381–385
[3] Akimoto H 2003 *Science* **302** 1716–1719
[4] Martin R V 2008 *Atmos. Environ.* **42** 7823–7843
[5] Lovett A M, Reid N M, Buckley J A, French J B and Cameron D M 1979 *Biol. Mass Spectrom.* **6** 91–97
[6] Thorpe M J, Balslev-Clausen D, Kirchner M S and Ye J 2008 *Opt. Express* **16** 2387–2397
[7] Wang C and Sahay P 2009 *Sensors* **9** 8230–8262
[8] Arslanov D D, Swinkels K, Cristescu S M and Harren F J M 2011 *Opt. Express* **19** 24078–24089
[9] Hodgkinson J and Tatam R P 2013 *Meas. Sci. Technol.* **24** 012004
[10] Swinehart D F 1962 *J. Chem. Educ.* **39** 333
[11] White J U 1942 *J. Opt. Soc. Am.* **32** 285–288
[12] Herriott D R and Schulte H J 1965 *Appl. Optics* **4** 883–889
[13] Thoma M L, Kaschow R and Hindelang F J 1994 *Shock Waves* **4** 51–53
[14] Mangold M, Tuzson B, Hundt M, Jgersk J, Looser H and Emmenegger L 2016 *J. Opt. Soc. Am. A* **33** 913–919
[15] Ayerden N P, de Graaf G and Wolffenbuttel R F 2016 *Opt. Express* **24** 2981–3002
[16] Ayerden N P, Ghaderi M, Enoksson P, de Graaf G and Wolffenbuttel R F 2016 *Sensor. Actuat. B-Chem.*
[17] Rushworth C M, Davies J, Cabral J T, Dolan P R, Smith J M and Vallance C 2012 *Chem. Phys. Lett.* **554** 1–14
[18] Noda T, Takao H, Yoshioka K, Oku N, Ashiki M, Sawada K, Matsumoto K and Ishida M 2006 *Sensor. Actuat. B-Chem.* **119** 245–250
[19] Tiggelaar R M, Veenstra T T, Sanders R G P, Gardeniers J G E, Elwenspoek M C and van den Berg A *Talanta* **56** 331–339
[20] Hendrickx N, Erps J V, Steenberge G V, Thienpont H and Daele P V 2007 *IEEE Photonic. Tech. L.* **19** 822–824
[21] Wang L, Wang X, Jiang W, Choi J, Bi H and Chen R 2005 *Appl. Phys. Lett.* **87** 141110
[22] Kagami M, Kawasaki A and Ito H 2001 *J. Lightwave Technol.* **19** 1949–1955
[23] Glebov A L, Roman J, Lee M G and Yokouchi K 2005 *IEEE Photonic. Tech. L.* **17** 1540–1542
[24] Maciel M J, Costa C G, Silva M F, Peixoto A C, Wolffenbuttel R F and Correia J H *Sensor. Actuat. A-Phys.* **242** 210–216
[25] Wang F, Liu F and Adibi A 2009 *Opt. Express* **17** 10514–10521
[26] Strandman C, Rosengren L, Elderstig H G A and Backlund Y 1995 *J. Microelectromech. S.* **4** 213–219
[27] Zubel I and Barycka I 1998 *Sensor. Actuat. A-Phys.* **70** 250–259
[28] Drago R, Danilo V, Uros A, Matej M and Slavko A 2005 *J. Micromech. Microeng.* **15** 1174
[29] Rola K, Ptasinski K, Zakrzewski A and Zubel I 2012 *Procedia Eng.* **47** 510–513
[30] Mattias V and Ylva B 1996 *J. Micromech. Microeng.* **6** 279
[31] Jun Hyun H, Shankar R and Chung-Hoon L 2013 *J. Micromech. Microeng.* **23** 055017
[32] Singh S S, Veerla S, Sharma V, Pandey A K and Pal P 2016 *J. Micromech. Microeng.* **26** 025012
[33] Kendall D L, Digges Iii T G, Eaton W P and Manginell R P 1994 *Opt. Eng.* **33** 3578–3588
[34] de Lima Monteiro D W, Akhzar-Mehr O, Sarro P M and Vdovin G 2003 *Opt. Express* **11** 2244–2252